ICI-Free Equalization in OFDM Systems with Blanking Preprocessing at the Receiver for Impulsive Noise Mitigation

Donatella Darsena, *Member, IEEE*, Giacinto Gelli, Fulvio Melito, and Francesco Verde, *Senior Member, IEEE*

***Abstract*—In this letter, we consider the problem of equalizing finite-impulse response (FIR) channels in orthogonal frequency-division multiplexing (OFDM) systems, which employ at the receiver a blanking nonlinearity to mitigate impulsive noise (IN). By exploiting the frequency redundancy associated with the presence of OFDM virtual carriers, we design a frequency-domain linear FIR equalizer that compensates for the intercarrier interference (ICI) generated by nonlinear preprocessing. Monte Carlo computer simulations, carried out assuming a Middleton Class A model for the IN, allows one to assess the error probability performance of the proposed equalizer.**

***Index Terms*—Blanking nonlinearity, intercarrier interference (ICI) suppression, linear equalization, Middleton Class A noise, orthogonal frequency-division multiplexing (OFDM) systems.**

I. Introduction

TRANSCEIVERS based on orthogonal frequency-division multiplexing (OFDM) have been widely adopted in several wired and wireless standards, including digital subscriber lines [1] and power line communications [2], digital audio [3] and video broadcasting [4], IEEE 802.11 [5] and 802.16 [6], and 3G/4G long term evolution [7]. Such a success is mainly due to the capability of OFDM transceivers to efficiently equalize finite-impulse response (FIR) frequency-selective channels [8]. Indeed, the use of Fast Fourier Transform (FFT) algorithms to perform discrete Fourier transform (DFT) and its inverse (IDFT), coupled with the insertion of a cyclic-prefix (CP), allows one to equalize the FIR channel by means of simple CP removal followed by one-tap frequency-domain equalization (FEQ), provided that the CP length exceeds channel dispersion.

In addition to additive white Gaussian noise (AWGN) and various transceiver implementation losses,[1] potential sources of performance degradation for OFDM systems operating over linear time-invariant channels include narrowband interference (NBI) and impulsive noise (IN). While NBI typically affects only a subset of subcarriers and can be rejected, e.g., by adding suitable constraints to the conventional zero-forcing (ZF) solution [9], [10], [11], [12], [13], [14], [15], [16], [17], [18], [19], [20], *asynchronous* non-Gaussian IN [21], [22], [23], [24], characterized by impulses occurring at the DFT input of the receiver with random arrivals, short duration, and high power, might corrupt *all* the subcarriers within an OFDM symbol and, hence, it is much more difficult to counteract.[2] This fact has recently motivated a vast bulk of research regarding IN characterization and mitigation in OFDM systems (see, e.g., [26], [27], [28], [29], [30], [31], [32], [33], [34]).

A simple strategy to mitigate IN in OFDM systems consists of using at the receiver, before the DFT, a memoryless nonlinearity preprocessor (e.g., clipping, blanking, or a combination thereof) [26], [27]. However, since blanking/clipping is a nonlinear sample-by-sample operation in the time-domain, it distorts the signal constellation and, even worse, destroys orthogonality among OFDM subcarriers, thus resulting into intercarrier interference (ICI) in the frequency-domain. To overcome such a problem, iterative cancellation techniques have been proposed in [28], [29], which nevertheless require *ad hoc* adjustments to avoid slow convergence. An alternative approach [33] is to introduce time diversity at the transmitter by interleaving multiple OFDM symbols after the IDFT and performing symbol-by-symbol blanking at the receiver. In this case, even though linear FIR equalization strategies, e.g., ZF or minimum mean-square error (MMSE) ones, can be used, channel estimation and synchronization must be acquired *before* deinterleaving. On the other hand, instead of employing nonlinear preprocessing at the receiver, it is possible to resort to advanced IN estimation and cancellation methods [30], [34], which exploit the sparsity features of noise in the time-domain. However, also in these cases, the resulting algorithms are iterative and, when compared to the conventional OFDM receiver, a significant computational burden is added.

In this letter, we show that, by exploiting the presence of *virtual carriers* (a solution present in several multicarrier standards), it is possible to design frequency-domain linear FIR

Manuscript received December 09, 2014; accepted January 27, 2015. Date of publication January 29, 2015; date of current version February 12, 2015. The associate editor coordinating the review of this manuscript and approving it for publication was Prof Antonio Marques.

D. Darsena is with the Department of Engineering, Parthenope University, Naples I-80143, Italy (e-mail: darsena@uniparthenope.it).

G. Gelli, F. Melito, and F. Verde are with the Department of Electrical Engineering and Information Technology, University Federico II, Naples I-80125, Italy (e-mail: gelli@unina.it; fulvio.melito@unina.it; f.verde@unina.it).

Color versions of one or more of the figures in this paper are available online at http://ieeexplore.ieee.org.

Digital Object Identifier 10.1109/LSP.2015.2398366

[1]Including time and carrier frequency offsets between the transmitter and the receiver, analog front-end in-phase/quadrature-phase (I/Q) imbalances, and insufficient CP length.

[2]Another type of non-Gaussian IN consists of impulses of longer duration that occur periodically in time (so-called *periodic* IN) [25].

equalizers for channels affected by IN, which are able to compensate for the ICI introduced by a blanking nonlinearity.[3] In particular, a sufficient condition ensuring the existence of such a FIR ICI-free solution is derived. Moreover, it is shown that, with respect to conventional ZF receivers (with or without blanking), a performance gain can be obtained for signal-to-noise ratio (SNR) values of practical interest, with an affordable increase in computational complexity.

A. Asynchronous IN Model

Although the design of the proposed ICI-free equalizer does not rely on specific assumptions about the IN, we briefly describe here the well-known asynchronous Middleton Class A (MCA) model [21]–[23], which will be employed in the numerical performance analysis. A MCA noise sample can be expressed as a complex random variable (RV) $x = g + i$, where g is zero-mean circular symmetric complex Gaussian thermal noise with variance σ_g^2, i.e., $g \in \mathcal{CN}(0, \sigma_g^2)$, whereas i models the non-Gaussian impulse noise with variance σ_i^2. The probability density function of x can be expressed as $p_x(z) = \sum_{n=0}^{+\infty} \alpha_n p_{x|n}(z|n)$, i.e., as a weighted sum of conditionally-Gaussian pdfs $p_{x|n}(z|n) \triangleq \pi^{-1}\sigma_n^{-2}\exp(-|z|^2/\sigma_n^2)$ $(z \in \mathbb{C})$, where $\alpha_n \triangleq e^{-\lambda}\lambda^n/n!$ is the probability that n noise pulses simultaneously occur. For any given $n \in \mathbb{N}$, the parameter σ_n^2 represents the conditional variance of x, which is given by $\sigma_n^2 = \sigma^2\beta_n$, where $\sigma^2 \triangleq \sigma_g^2 + \sigma_i^2$ is the variance of x, whereas $\beta_n \triangleq (n\lambda^{-1} + \Gamma)/(1+\Gamma)$, with $\lambda > 0$ the *impulsive index* and $\Gamma \triangleq \sigma_g^2/\sigma_i^2 > 0$ the *Gaussian ratio*. The two parameters λ and Γ control the degree of impulsiveness of the noise: for $\lambda \ll 1$, the noise becomes more and more impulsive; for $\lambda \geq 1$, the noise tends to be Gaussian. Similarly, for small values of Γ, the noise becomes more impulsive, while it tends to be Gaussian for large values of Γ. Typically, it is assumed that $\Gamma \ll 1$ (see, e.g., [28]).

II. OFDM System Model

We consider a single-user OFDM system employing M subcarriers, M_{uc} of which are utilized, whereas the remaining $M_{\text{vc}} \triangleq M - M_{\text{uc}} > 0$ ones are virtual carriers (VCs). The discrete-time channel between the transmitter and the receiver is modeled as a causal FIR filter with impulse response $h(n)$ $(n \in \mathbb{Z})$, whose order L_h does not exceed the CP length L_{cp}, with $h(0), h(L_h) \neq 0$. Perfect symbol and carrier-frequency synchronization between the transmitter and the receiver is assumed, and channel state information is known only at the receiver via training, but is unknown at the transmitter.

Let $\mathbf{s} \in \mathbb{C}^{M_{\text{uc}}}$ be the data block to be transmitted,[4] we assume that: **(a1)** $\mathbf{s}$ is a zero-mean circularly symmetric complex random vector, with correlation matrix $\mathbb{E}[\mathbf{s}\mathbf{s}^{\text{H}}] = \mathbf{I}_{M_{\text{uc}}}$, and whose entries assume independent and identically distributed (i.i.d.) equiprobable values, e.g., belonging to a quadrature amplitude modulation (QAM) constellation. Let $\mathcal{J}_{\text{uc}} \triangleq \{q_0, q_1, \ldots, q_{M_{\text{uc}}-1}\} \subset \mathcal{J} \triangleq \{0, 1, \ldots, M-1\}$ collect all the indices of the used subcarriers, the symbol block $\mathbf{s}$ is first processed by the full-column rank matrix $\mathbf{\Theta} \in \mathbb{R}^{M \times M_{\text{uc}}}$, which inserts the VCs in the arbitrary positions $\mathcal{J}_{\text{vc}} \triangleq \mathcal{J} - \mathcal{J}_{\text{uc}}$. By construction, it results that $\mathbb{E}[||\mathbf{\Theta}\mathbf{s}||^2] = 1$. Before being transmitted, the entries of $\mathbf{\Theta}\mathbf{s} \in \mathbb{C}^M$ are subject to conventional OFDM processing, encompassing M-point IDFT followed by CP insertion.

At the receiver, after discarding the CP, the time-domain block can be written [8] as

$$\mathbf{r} = \mathbf{H}\mathbf{W}_{\text{IDFT}}\mathbf{\Theta}\mathbf{s} + \mathbf{w} \tag{1}$$

where $\mathbf{H} \in \mathbb{C}^{M \times M}$ is a circulant matrix, whose first column is $[h(0), \ldots, h(L_h), 0, \ldots, 0]^{\text{T}}$, $\mathbf{W}_{\text{IDFT}} \in \mathbb{C}^{M \times M}$ is the unitary symmetric IDFT matrix,[5] and $\mathbf{w} \in \mathbb{C}^M$ models the additive noise. It is assumed that: **(a2)** the vector $\mathbf{w} \triangleq [w_0, w_1, \ldots, w_{M-1}]^{\text{T}}$ is independent of $\mathbf{s}$, and its elements are i.i.d. zero-mean RVs with variance $\sigma^2 \triangleq \mathbb{E}[|w_m|^2]$, modeled e.g. as MCA RVs with parameters Γ and λ.

By resorting to standard eigenstructure concepts [35], one has $\mathbf{H} = \mathbf{W}_{\text{IDFT}}\boldsymbol{\mathcal{H}}\mathbf{W}_{\text{DFT}}$ in (1), where the diagonal entries of $\boldsymbol{\mathcal{H}} \triangleq \text{diag}(H_0, H_1, \ldots, H_{M-1})$ are the values of the transfer function $H(z) \triangleq \sum_{n=0}^{L_h} h(n) z^{-n}$ evaluated at the subcarriers $z_m \triangleq \exp[j(2\pi/M)m]$, i.e., $H_m = H(z_m)$, $\forall m \in \mathcal{J}$. We assume that: **(a3)** the channel transfer function $H(z)$ has no zero on the used subcarriers, i.e., $H_m \neq 0$, $\forall m \in \mathcal{J}_{\text{uc}}$.

III. ICI Analysis of Sample-by-sample Blanking

To mitigate the adverse effects of IN, a common strategy is to use sample-by-sample blanking preprocessing [26], [27] in the time-domain, before the conventional OFDM equalizer (i.e., before DFT and FEQ), aimed at discarding those samples of $\mathbf{r}$ that are most contaminated by IN.

Let r_m be the mth $(m \in \mathcal{J})$ sample of $\mathbf{r}$ and $\xi > 0$ denote a suitable threshold, the output of the blanking nonlinearity is $\tilde{y}_m = r_m$ if $|r_m| \leq \xi$, $\tilde{y}_m = 0$ otherwise. Let $\mathcal{B} \triangleq \{m \in \mathcal{J} : |r_m| > \xi\} = \{m_1, m_2, \ldots, m_{|\mathcal{B}|}\}$ denote the subset collecting all the indices of the blanked entries of $\mathbf{r}$; the complement of $\mathcal{B}$ with respect to $\mathcal{J}$ is denoted by $\overline{\mathcal{B}} = \{\overline{m}_1, \overline{m}_2, \ldots, \overline{m}_{|\overline{\mathcal{B}}|}\}$. The input-output relationship of the blanking preprocessor is $\tilde{\mathbf{y}} \triangleq [\tilde{y}_0, \tilde{y}_1, \ldots, \tilde{y}_{M-1}]^{\text{T}} = (\mathbf{I}_M - \mathbf{B})\,\mathbf{r}$, where $\mathbf{B} \triangleq \text{diag}(b_0, b_1, \ldots, b_{M-1})$, with $b_m = 1$ for $m \in \mathcal{B}$, $b_m = 0$ otherwise.

Taking into account (1) and the eigenstructure of $\mathbf{H}$, after DFT one obtains the frequency-domain block $\mathbf{y} \triangleq \mathbf{W}_{\text{DFT}}\tilde{\mathbf{y}} = \mathbf{C}\boldsymbol{\mathcal{H}}\mathbf{\Theta}\mathbf{s} + \mathbf{v}$, where $\mathbf{C} \triangleq \mathbf{W}_{\text{DFT}}(\mathbf{I}_M - \mathbf{B})\mathbf{W}_{\text{IDFT}} \in \mathbb{C}^{M \times M}$ and $\mathbf{v} \triangleq \mathbf{W}_{\text{DFT}}(\mathbf{I}_M - \mathbf{B})\mathbf{W} \in \mathbb{C}^M$. It can be verified that $\mathbf{C}$ is a circulant matrix, whose diagonal entries $\{\mathbf{C}\}_{m,m}$ for each $m \in \mathcal{J}$ are equal to $\{\mathbf{C}\}_{m,m} = 1 - |\mathcal{B}|/M = 1 - (M - |\overline{\mathcal{B}}|)/M = |\overline{\mathcal{B}}|/M$, where $|\mathcal{B}|$ and $|\overline{\mathcal{B}}|$ denote the cardinality of $\mathcal{B}$ and $\overline{\mathcal{B}}$, respectively. Consequently, vector $\mathbf{y}$ can be rewritten as

$$\mathbf{y} = \underbrace{\frac{|\overline{\mathcal{B}}|}{M}\boldsymbol{\mathcal{H}}\mathbf{\Theta}\mathbf{s}}_{(a)} + \underbrace{\left(\mathbf{C} - \frac{|\overline{\mathcal{B}}|}{M}\mathbf{I}_M\right)\boldsymbol{\mathcal{H}}\mathbf{\Theta}\mathbf{s}}_{(b)} + \mathbf{v}. \tag{2}$$

[3] The proposed approach can be extended to other memoryless nonlinearities [27], e.g., clipping or combination of blanking and clipping.

[4] Since all the considered processing is on a symbol-by-symbol basis, for the sake of notation simplicity, we avoid indicating the functional dependence on the symbol interval index.

[5] Its inverse $\mathbf{W}_{\text{DFT}} \triangleq \mathbf{W}_{\text{IDFT}}{}^{-1} = \mathbf{W}_{\text{IDFT}}^{*}$ is the DFT matrix.

The latter equation shows that the adverse effect of blanking is twofold [29]: (i) reduction of the signal amplitude by a factor $|\overline{\mathcal{B}}|/M$; (ii) introduction of ICI, due to departure of $\mathbf{C}$ from a scaled identity matrix. Indeed, if no entry of $\mathbf{r}$ is blanked, then $|\overline{\mathcal{B}}| = M$ and $\mathbf{C} = \mathbf{I}_M$. In Section IV, we show that these undesired effects of the nonlinearity can be compensated for by a frequency-domain linear FIR equalizer.

IV. Frequency-domain FIR ICI-free Equalization

Consider the problem of recovering the transmitted block $\mathbf{s}$ from the blanking preprocessor output $\mathbf{y}$ after DFT. To this purpose, we employ a frequency-domain linear FIR equalizer, defined by the input-output relationship $\mathbf{x} = \mathbf{F}\mathbf{y}$, with $\mathbf{F} \in \mathbb{C}^{M_{\rm uc} \times M}$, followed by a minimum-distance decision device. The ICI-free condition leads to the matrix equation $\mathbf{F}\mathbf{C}\boldsymbol{\mathcal{H}}\boldsymbol{\Theta} = \mathbf{I}_{M_{\rm uc}}$. Such an equation is consistent (i.e., it admits at least one solution) if and only if (iff) $(\mathbf{C}\boldsymbol{\mathcal{H}}\boldsymbol{\Theta})^{-}(\mathbf{C}\boldsymbol{\mathcal{H}}\boldsymbol{\Theta}) = \mathbf{I}_{M_{\rm uc}}$, with $(\cdot)^{-}$ denoting the generalized (1)-inverse [36]. This condition is fulfilled[6] if $\mathbf{C}\boldsymbol{\mathcal{H}}\boldsymbol{\Theta}$ is full-column rank, i.e., $\text{rank}(\mathbf{C}\boldsymbol{\mathcal{H}}\boldsymbol{\Theta}) = M_{\rm uc}$. Under this assumption, the *minimal norm* [36] solution of $\mathbf{F}\mathbf{C}\boldsymbol{\mathcal{H}}\boldsymbol{\Theta} = \mathbf{I}_{M_{\rm uc}}$ is given by $\mathbf{F}_{\text{ICI}-\text{free}} = (\mathbf{C}\boldsymbol{\mathcal{H}}\boldsymbol{\Theta})^{\dagger}$, with $(\cdot)^{\dagger}$ denoting the Moore-Penrose generalized inverse [36].

A. Sufficient Condition for the Existence of ICI-free Solutions

We investigate whether $\text{rank}(\mathbf{C}\boldsymbol{\mathcal{H}}\boldsymbol{\Theta}) = M_{\rm uc}$ is satisfied, which is a sufficient condition for the existence of ICI-free solutions. To this aim, we provide the following Theorem.

Theorem 1: (Existence of ICI-free solutions): The matrix $\mathbf{C}\boldsymbol{\mathcal{H}}\boldsymbol{\Theta}$ is full-column rank iff $[\boldsymbol{\mathcal{H}}\boldsymbol{\Theta}, \mathbf{W}_{\rm DFT}\boldsymbol{\Psi}] \in \mathbb{C}^{M \times (M_{\rm uc} + |\mathcal{B}|)}$ is full-column rank, where $\boldsymbol{\Psi} \triangleq [\mathbf{1}_{m_1}, \mathbf{1}_{m_2}, \ldots, \mathbf{1}_{m_{|\mathcal{B}|}}] \in \mathbb{R}^{M \times |\mathcal{B}|}$, with $\mathbf{1}_m \in \mathbb{R}^M$ denoting the $(m+1)$th column of $\mathbf{I}_M$.

Proof: Since the matrix $\mathbf{W}_{\rm DFT}$ is nonsingular, it results that $\text{rank}(\mathbf{C}\boldsymbol{\mathcal{H}}\boldsymbol{\Theta}) = \text{rank}[(\mathbf{I}_M - \mathbf{B})\mathbf{W}_{\rm IDFT}\boldsymbol{\mathcal{H}}\boldsymbol{\Theta}]$. Moreover, by virtue of assumption **(a3)**, one has $\text{rank}(\boldsymbol{\mathcal{H}}\boldsymbol{\Theta}) = M_{\rm uc}$, which implies that $\text{rank}(\mathbf{W}_{\rm IDFT}\boldsymbol{\mathcal{H}}\boldsymbol{\Theta}) = M_{\rm uc}$, since $\mathbf{W}_{\rm IDFT}$ is a nonsingular matrix. The matrix $(\mathbf{I}_M - \mathbf{B})\mathbf{W}_{\rm IDFT}\boldsymbol{\mathcal{H}}\boldsymbol{\Theta} \in \mathbb{C}^{M \times M_{\rm uc}}$ is full-column rank iff [36] $\mathcal{N}(\mathbf{I}_M - \mathbf{B}) \cap \mathcal{R}(\mathbf{W}_{\rm IDFT}\boldsymbol{\mathcal{H}}\boldsymbol{\Theta}) = \{\mathbf{0}_M\}$. By construction, the mth diagonal entry of $\mathbf{I}_M - \mathbf{B}$ is zero for each $m \in \mathcal{B}$ and, thus, $\text{rank}(\mathbf{I}_M - \mathbf{B}) = M - |\mathcal{B}| = |\overline{\mathcal{B}}|$. Recalling that m_i denotes the ith element of $\mathcal{B}$, for $i \in \{1, 2, \ldots, |\mathcal{B}|\}$, an arbitrary vector $\boldsymbol{\mu} \in \mathbb{C}^M$ belongs to $\mathcal{N}(\mathbf{I}_M - \mathbf{B})$ iff there exists a vector $\boldsymbol{\beta} \in \mathbb{C}^{|\mathcal{B}|}$ such that $\boldsymbol{\mu} = \boldsymbol{\Psi}\boldsymbol{\beta}$, with $\boldsymbol{\Psi} \triangleq [\mathbf{1}_{m_1}, \mathbf{1}_{m_2}, \ldots, \mathbf{1}_{m_{|\mathcal{B}|}}] \in \mathbb{R}^{M \times |\mathcal{B}|}$, where $\mathbf{1}_m \in \mathbb{R}^M$ is the $(m+1)$th column of $\mathbf{I}_M$. Hence, an arbitrary vector $\boldsymbol{\mu} \in \mathcal{N}(\mathbf{I}_M - \mathbf{B})$ also belongs to the subspace $\mathcal{R}(\mathbf{W}_{\rm IDFT}\boldsymbol{\mathcal{H}}\boldsymbol{\Theta})$ iff there exists a vector $\boldsymbol{\alpha} \in \mathbb{C}^{M_{\rm uc}}$ such that $\boldsymbol{\Psi}\boldsymbol{\beta} = \mathbf{W}_{\rm IDFT}\boldsymbol{\mathcal{H}}\boldsymbol{\Theta}\boldsymbol{\alpha}$. As a consequence, condition $\mathcal{N}(\mathbf{I}_M - \mathbf{B}) \cap \mathcal{R}(\mathbf{W}_{\rm IDFT}\boldsymbol{\mathcal{H}}\boldsymbol{\Theta}) = \{\mathbf{0}_M\}$ holds iff the system of equations $\boldsymbol{\mathcal{H}}\boldsymbol{\Theta}\boldsymbol{\alpha} - \mathbf{W}_{\rm DFT}\boldsymbol{\Psi}\boldsymbol{\beta} = \mathbf{0}_M$ admits the unique solution $\boldsymbol{\alpha} = \mathbf{0}_{M_{\rm uc}}$ and $\boldsymbol{\beta} = \mathbf{0}_{|\mathcal{B}|}$. It can be seen [35] that this happens iff the matrix $[\boldsymbol{\mathcal{H}}\boldsymbol{\Theta}, \mathbf{W}_{\rm DFT}\boldsymbol{\Psi}] \in \mathbb{C}^{M \times (M_{\rm uc} + |\mathcal{B}|)}$ turns out to be full-column rank. ■

Some remarks are now in order. First, perfect ICI suppression may not be achieved, i.e., $\mathbf{C}\boldsymbol{\mathcal{H}}\boldsymbol{\Theta}$ might not be full-column rank, even if the channel transfer function $H(z)$ has no zero on the used subcarriers [see assumption **(a3)**]. This is due to the fact that the blanking preprocessor introduces ICI in the frequency-domain signal. Only when no entry of $\mathbf{r}$ is blanked, assumption **(a3)** is sufficient for assuring the existence of ICI-free solutions. Second, the fact that some entries of $\mathbf{r}$ are blanked does not prevent perfect ICI compensation. This result stems from the fact that the blanking preprocessor operates in the time-domain (i.e., before the DFT), where each entry of $\mathbf{r}$ is a (noisy) linear combination of all the entries of $\mathbf{s}$. Therefore, if the (m_i)-th sample is blanked, i.e., $b_{m_i} = 1$, the vector $\mathbf{s}$ can still be recovered from the other entries of $\mathbf{r}$. Third, condition $\text{rank}(\mathbf{C}\boldsymbol{\mathcal{H}}\boldsymbol{\Theta}) = M_{\rm uc}$ amounts to $\text{rank}([\boldsymbol{\mathcal{H}}\boldsymbol{\Theta}, \mathbf{W}_{\rm DFT}\boldsymbol{\Psi}]) = M_{\rm uc} + |\mathcal{B}|$, which necessarily requires that $M \geq M_{\rm uc} + |\mathcal{B}|$ or, equivalently, $M_{\rm vc} \geq |\mathcal{B}|$. Thus, the number $M_{\rm vc}$ of VCs also represents the maximum number of entries of $\mathbf{r}$ that can be blanked without preventing perfect ICI compensation.

Finally, Theorem 1 does not allow one to determine the threshold ξ (or, equivalently, the blanking subset $\mathcal{B}$), whose choice nevertheless affects the symbol-error-rate (SER) performance of the receiver. Since closed-form analytical evaluation of SER as a function of ξ is a challenging problem,[7] we explore the impact of ξ on SER performance and discuss its choice in Section V by numerical experiments.

B. Computational Complexity

The computational complexity of the $\mathbf{F}_{\text{ICI}-\text{free}}$ equalizer is dominated by calculation of the Moore-Penrose generalized inverse of $\mathbf{C}\boldsymbol{\mathcal{H}}\boldsymbol{\Theta}$. To evaluate such a complexity, observe that the matrix $\mathbf{C}\boldsymbol{\mathcal{H}}\boldsymbol{\Theta}$ is obtained from $\mathbf{C}\boldsymbol{\mathcal{H}} = [\boldsymbol{\zeta}_0, \boldsymbol{\zeta}_1, \ldots, \boldsymbol{\zeta}_{M-1}]$ by picking its columns $\boldsymbol{\zeta}_q \in \mathbb{C}^M$ located on the used subcarrier positions, i.e., for $q \in \mathcal{J}_{\rm uc}$. It results that $\boldsymbol{\zeta}_q = H_q \sum_{\overline{m} \in \overline{\mathcal{B}}} z_{q\overline{m}} \boldsymbol{\chi}_{\overline{m}}$, where $\boldsymbol{\chi}_{\overline{m}} \triangleq (1/M)[1, z_{\overline{m}}, z_{2\overline{m}} \ldots, z_{(M-1)\overline{m}}]^{\rm H} \in \mathbb{C}^M$. Let $\mathbf{e}_q \triangleq [z_{q\overline{m}_1}, z_{q\overline{m}_2} \ldots, z_{q\overline{m}_{|\overline{\mathcal{B}}|}}]^{\rm T} \in \mathbb{C}^{|\overline{\mathcal{B}}|}$, one has $\mathbf{C}\boldsymbol{\mathcal{H}}\boldsymbol{\Theta} = \boldsymbol{\Omega}\mathbf{E}\boldsymbol{\mathcal{H}}_{\rm uc}$, with $\boldsymbol{\Omega} \triangleq [\boldsymbol{\chi}_{\overline{m}_1}, \boldsymbol{\chi}_{\overline{m}_2}, \ldots, \boldsymbol{\chi}_{\overline{m}_{|\overline{\mathcal{B}}|}}] \in \mathbb{C}^{M \times |\overline{\mathcal{B}}|}$, $\mathbf{E} \triangleq [\mathbf{e}_{q_0}, \mathbf{e}_{q_1}, \ldots, \mathbf{e}_{q_{M_{\rm uc}-1}}] \in \mathbb{C}^{|\overline{\mathcal{B}}| \times M_{\rm uc}}$, and $\boldsymbol{\mathcal{H}}_{\rm uc} \triangleq \text{diag}(H_{q_0}, H_{q_1}, \ldots, H_{q_{M_{\rm uc}-1}})$. Since $\boldsymbol{\mathcal{H}}_{\rm uc}$ is nonsingular by virtue of assumption **(a3)** and $\boldsymbol{\Omega}\mathbf{E}$ is full-column rank by construction, i.e., rank $(\boldsymbol{\Omega}\mathbf{E}) = M_{\rm uc}$, it results [36] that $\mathbf{F}_{\text{ICI}-\text{free}} = \boldsymbol{\mathcal{H}}_{\rm uc}{}^{-1}(\boldsymbol{\Omega}\mathbf{E})^{\dagger} = M\boldsymbol{\mathcal{H}}_{\rm uc}{}^{-1}\mathbf{E}^{\dagger}\boldsymbol{\Omega}^{\rm H}$, where we additionally used the fact that $\boldsymbol{\Omega}^{\rm H}\boldsymbol{\Omega} = (1/M)\mathbf{I}_{|\overline{\mathcal{B}}|}$.

Compared to the conventional OFDM receiver, the increase in computational complexity for the proposed ICI-free equalizer is due to the calculus of $\mathbf{E}^{\dagger}$. It can be verified that $\mathbf{E}$ is a polynomial Vandermonde matrix [39] with basis polynomials $P_j(x) = x^{q_j}$, for $x \in \mathbb{C}$ and $j \in \{0, 1, \ldots, M_{\rm uc} - 1\}$, and node points $t_i = z_{m_i}$, for $j \in \{1, 2, \ldots, |\overline{\mathcal{B}}|\}$.[8] Thus, the matrix $\mathbf{E}^{\dagger}$ can be calculated [39] by special fast or superfast algorithms in $\mathcal{O}(M^2)$ or $\mathcal{O}(M \log^2(M))$ floating point operations, respectively.

[6]Also the performance of the MMSE equalizer depends on the existence of ICI-free solutions: if $\text{rank}(\mathbf{C}\boldsymbol{\mathcal{H}}\boldsymbol{\Theta}) \neq M_{\rm uc}$, the error probability performance curve of the MMSE equalizer exhibits a floor when $\sigma^2 \to 0$ [37], [38].

[7]In principle, following [26], [27], one may choose ξ so as to maximize the signal-to-interference-plus-noise ratio (SINR) at the equalizer output, which is simpler to evaluate. However, since the IN is non-Gaussian, SINR maximization is no longer equivalent to SER minimization.

[8]According to Theorem 1, one has $|\overline{\mathcal{B}}| \geq M_{\rm uc}$ and rank $(\mathbf{E}) = M_{\rm uc}$.

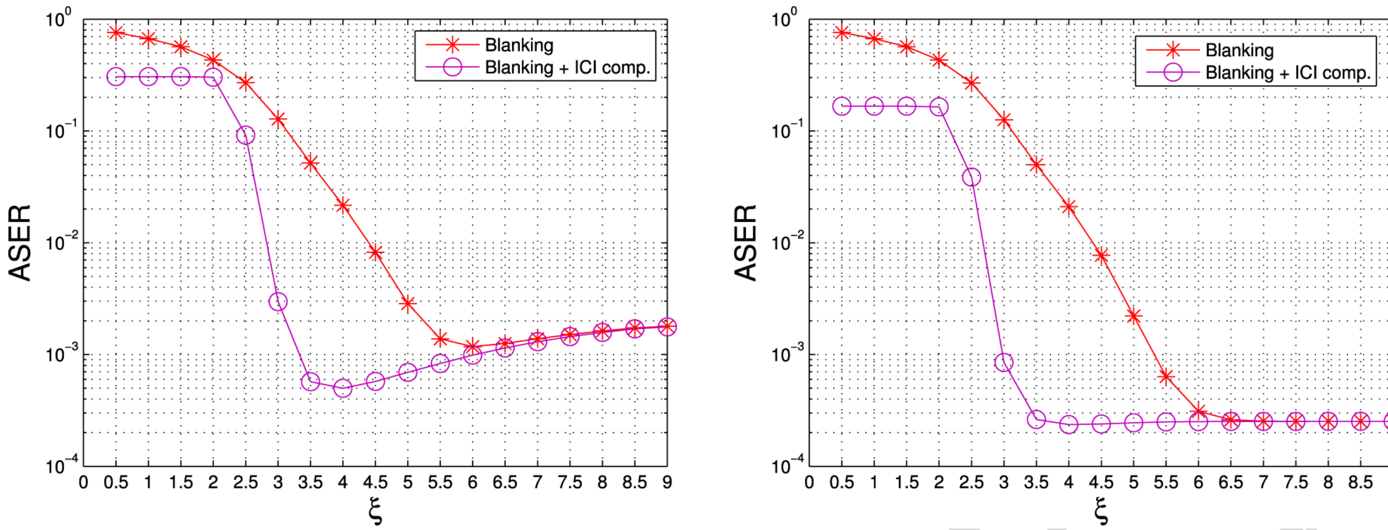

Fig. 1. ASER versus ξ with SNR equal to 15 dB (left-side plot) and 25 dB (right-side plot).

V. Numerical Performance Analysis

The average SER (ASER) performance of the proposed ICI-free receiver (referred to as "Blanking + ICI comp.") was assessed by means of Monte Carlo computer simulations. As a comparison, we also evaluated the ASER performance of: (i) the receiver with blanking nonlinearity followed by conventional ZF equalization, i.e., $\mathbf{F}_{\text{zf}} = (\boldsymbol{\mathcal{H}}\boldsymbol{\Theta})^{\dagger}$ (referred to as "Blanking"); (ii) the conventional OFDM receiver without any nonlinearity preprocessing and ZF equalization (referred to as "Conventional"). With reference to the proposed equalizer, according to Theorem 1, only the M_{vc} entries of $\mathbf{r}$ with largest magnitudes are blanked if $|\mathcal{B}| > M_{\text{vc}}$.

We considered an OFDM system with $M = 32$ subcarriers and a CP length $L_{\text{cp}} = 8$. The system employs $M_{\text{vc}} = 8$ VCs, all located at the edges of the OFDM spectrum, and Gray-labeled 4-QAM signaling for the $M_{\text{uc}} = 24$ utilized subcarriers.[9] The channel impulse response was chosen according to the channel model HiperLAN/2 A (see [40] for details). The MCA impulsive noise was generated by using a modified version of the Matlab toolbox in [41]. We considered a *highly-impulsive* noise scenario with $\lambda = 10^{-3}$ and $\Gamma = 10^{-1}$.

Fig. 1 reports the performance of the two receivers with blanking as a function of the threshold ξ, with SNR $\triangleq 1/\sigma^2 \in \{15, 25\}$ dB. Results show that, as expected, the performance of both receivers depends on the value of the blanking threshold. However, the "Blanking + ICI comp." receiver outperforms the "Blanking" one for all the considered values of ξ, except for very large values of ξ when the entries of $\mathbf{r}$ are not blanked with high probability and, then, the ICI-free equalizer $\mathbf{F}_{\text{ICI-free}}$ boils down to the ZF matrix $\mathbf{F}_{\text{zf}}$.

The ASER performances of all the considered receivers are depicted in Fig. 2 as a function of the SNR. With regard to the receivers employing blanking, we chose the value of ξ minimizing the ASER, for each SNR value. It can be seen that, compared to the conventional OFDM receiver, employing a blanking preprocessing allows one to remarkably improve performances, except for large values of the SNR, for which blanking becomes unlikely and, thus, all the three receivers tend to coincide. Remarkably, the "Blanking+ICI comp." receiver outperforms the "Blanking" one for SNR values of practical interest, ranging from 10 to 20 dB. For instance, for an ASER value of 10^{-3}, the "Blanking + ICI comp." receiver ensures an SNR gain of about 6 dB with respect to the "Blanking" and "Conventional" ones.

[9]We performed simulations using a 16-QAM constellation, whose ASER curves are not reported since they show trends similar to the 4-QAM case.

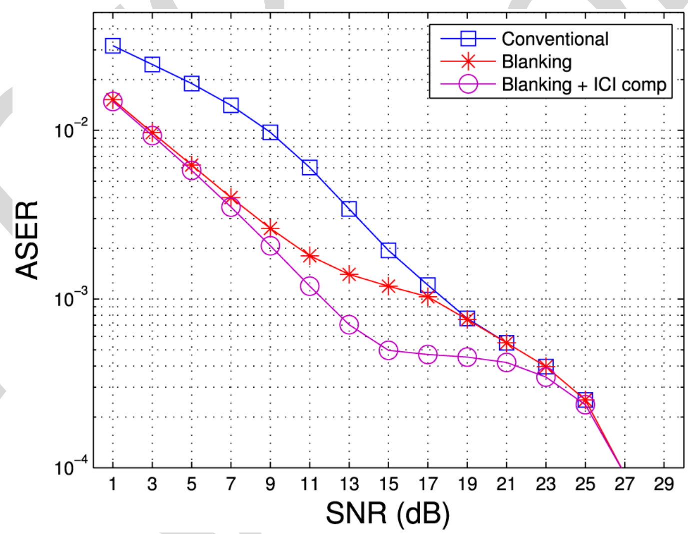

Fig. 2. ASER versus SNR with ξ optimally chosen for each SNR value.

VI. Conclusions

By exploiting the redundancy arising from the insertion of VCs in the OFDM signal, we showed that closed-form FIR ICI-free compensation in OFDM receivers, which employ blanking nonlinearity processing to counteract IN, is still feasible. In this case, significant performance gains are obtained with a minor modification of the conventional ZF equalizer.

REFERENCES

[1] T. Starr, M. Sorbara, J. M. Cioffi, and P. J. Silverman, *DSL Advances*. Upper Saddle River, NJ, USA: Prentice Hall Professional, 2003.

[2] H. Hrasnica, A. Haidine, and R. Lehnert, *Broadband Powerline Communications*. Hoboken, NJ, USA: Wiley, 2004.

[3] Radio broadcasting systems; Digital audio broadcasting (DAB) to mobile, portable and fixed receivers, ETS Standard 300 401, 1995.

[4] Digital video broadcasting (DVB); Framing structure, channel coding and modulation for digital terrestrial television, ETSI Std. EN 300 744 v1.6.1, 2008.

[5] B. O'Hara and A. Petrick, *The IEEE 802.11 Handbook: A Designer's Companion*. Piscataway, NJ, USA: IEEE Standards, 2005.

[6] IEEE Standard for local and metropolitan area networks Part 16: Air interface for broadband wireless access systems Amendment 3: Advanced air interface, IEEE Std. 802.16 m, 2011.

[7] LTE; Evolved universal terrestrial radio access (E-UTRA) and evolved universal terrestrial radio access network (E-UTRAN); Overall description, 3GPP Std. TS 36.300, 2011.

[8] Z. Wang and G. B. Giannakis, "Wireless multicarrier communications–where fourier meets shannon," *IEEE Signal Process. Mag.*, vol. 17, no. 3, pp. 29–48, May 2000.

[9] D. Darsena, G. Gelli, L. Paura, and F. Verde, "Widely-linear equalization and blind channel identification for interference-contaminated multicarrier systems," *IEEE Trans. Signal Process*, vol. 53, pp. 1163–1177, Mar. 2005.

[10] S. H. Müller-Weinfurtner, "Optimum Nyquist windowing in OFDM receivers," *IEEE Trans. Commun.*, vol. 49, pp. 417–420, Mar. 2002.

[11] D. Darsena, G. Gelli, L. Paura, and F. Verde, "NBI-resistant zero-forcing equalizers for OFDM systems," *IEEE Commun. Lett.*, vol. 9, pp. 744–746, Aug. 2005.

[12] A. J. Redfern, "Receiver window design for multicarrier communication systems," *IEEE J. Sel. Areas Commun.*, vol. 20, pp. 1029–1036, Jun. 2002.

[13] D. Darsena, G. Gelli, L. Paura, and F. Verde, "A constrained maximum-SINR NBI-resistant receiver for OFDM systems," *IEEE Trans. Signal Process.*, vol. 55, pp. 3032–3047, Jun. 2007.

[14] K. Van Acker, G. Leus, M. Moonen, O. van de Wiel, and T. Pollet, "Per tone equalization for DMT-based systems," *IEEE Trans. Commun.*, vol. 49, no. pp, pp. 109–119, Jan. 2001.

[15] K. Van Acker, T. Pollet, G. Leus, and M. Moonen, "Combination of per tone equalization and windowing in DMT-receivers," *Signal Process.*, vol. 81, pp. 1571–1579, Aug. 2001.

[16] D. Darsena, "Successive narrowband interference cancellation for OFDM systems," *IEEE Commun. Lett.*, vol. 11, pp. 73–75, Jan. 2007.

[17] K. Vanbleu, M. Moonen, and G. Leus, "Linear and decision-feedback per tone equalization for DMT-based transmission over IIR channels," *IEEE Trans. Signal Process.*, vol. 54, pp. 258–273, Jan. 2006.

[18] D. Darsena, G. Gelli, and F. Verde, "Universal linear precoding for NBI-proof widely-linear equalization in MC systems," *EURASIP J. Wireless Commun. Netw., Special Issue on Multicarrier Systems*, pp. 1–13, 2008, ID 321450.

[19] S. Trautmann and N. J. Fliege, "A new equalizer for multitone systems without guard time," *IEEE Commun. Lett.*, vol. 6, pp. 34–36, Jan. 2002.

[20] D. Darsena and F. Verde, "Successive NBI cancellation using soft decisions for OFDM systems," *IEEE Signal Process. Lett.*, vol. 15, pp. 873–876, 2008.

[21] D. Middleton, "Statistical-physical models of electromagnetic interference," *IEEE Trans. Electromagn. Compat.*, vol. 19, pp. 106–127, Aug. 1977.

[22] A. D. Spaulding and D. Middleton, "Optimum reception in the impulse interference environment–part I: Coherent detection," *IEEE Trans. Commun.*, vol. 25, pp. 910–923, Sep. 1977.

[23] D. Middleton, "Procedure for determining the parameters of a first-order canonical models of class A and class B electromagnetic interference," *IEEE Trans. Electromagn. Compat.*, vol. 21, pp. 190–208, Aug. 1979.

[24] P. A. Delaney, "Signal detection in multivariate class-A interference," *IEEE Trans. Commun.*, vol. 43, pp. 365–373, Feb. 2006.

[25] M. Nassar, A. Dabak, I. Kim, T. Pande, and B. L. Evans, "Cyclostationary noise modeling in narrowband powerline communication for smart grid application," in *Proc. IEEE Int. Conf. on Acoustics, Speech and Sig. Proc.*, Kyoto, Japan, Mar. 2012, pp. 3089–3092.

[26] S. V. Zhidkov, "Performance analysis and optimization of OFDM receiver with blanking nonlinearity in impulsive noise environment," *IEEE Trans. Veh. Technol.*, vol. 55, pp. 234–242, Jan. 2006.

[27] S. V. Zhidkov, "Analysis and comparison of several simple impulse noise mitigation schemes for OFDM receivers," *IEEE Trans. Commun.*, vol. 56, pp. 5–9, Jan. 2008.

[28] A. Mengi and A. Vinck, "Successive impulse noise suppression in OFDM," in *Proc. 2010 IEEE Int. Symp. Power Line Communications and Its Applications*, Rio de Janeiro, Brazil, Mar. 2010, pp. 33–37.

[29] C.-H. Yih, "Iterative interference cancellation for OFDM signals with blanking nonlinearity in impulsive noise channels," *IEEE Signal Process. Lett.*, vol. 19, pp. 147–150, Mar. 2012.

[30] J. Lin, M. Nassar, and B. L. Evans, "Impulsive noise mitigation in powerline communications using sparse Bayesian learning," *IEEE J. Sel. Areas Commun.*, vol. 31, pp. 1172–1183, Jul. 2013.

[31] R. Savoia and F. Verde, "Performance analysis of distributed space-time block coding schemes in Middleton class a noise," *IEEE Trans. Veh. Technol.*, vol. 62, pp. 2579–2595, Jul. 2013.

[32] D. Darsena, G. Gelli, F. Melito, and F. Verde, "Impulse noise mitigation for MIMO-OFDM wireless networks with linear equalization," in *Proc. IEEE Int. Workshop on Measurements and Networking (M&N)*, Naples, Italy, Oct. 2013, pp. 94–99.

[33] M. Mirahmadi, A. Al-Dweik, and A. Shami, "BER reduction of OFDM based broadband communication systems over multipath channels with impulsive noise," *IEEE Trans. Commun.*, vol. 61, pp. 4602–4615, Nov. 2013.

[34] T. Y. Al-Naffouri, A. A. Quadeer, and G. Caire, "Impulsive noise estimation and removal for OFDM systems," *IEEE Trans. Commun.*, vol. 62, pp. 976–989, Mar. 2014.

[35] R. A. Horn and C. R. Johnson, *Matrix Analysis*. Cambridge, U.K.: Cambridge Univ. Press, 1990.

[36] A. Ben-Israel and T. N. E. Greville, *Generalized Inverses*. New York, NY, USA: Springer-Verlag, 2002.

[37] F. Verde, "Subspace-based blind multiuser detection for quasi-synchronous MC-CDMA systems," *IEEE Signal Process. Lett.*, vol. 11, pp. 621–624, Jul. 2004.

[38] A. S. Cacciapuoti, G. Gelli, and F. Verde, "FIR zero-forcing multiuser detection and code designs for downlink MC-CDMA," *IEEE Trans. Signal Process.*, vol. 55, pp. 4737–4751, Oct. 2007.

[39] V. Y. Pan, *Structured Matrices and Polynomials: Unified Superfast Algorithms*. Boston, MA, USA: Birkhäuser, 2001.

[40] ETSI Normalization Committee, Channel models for HIPERLAN/2 in different indoor scenarios, [Online]. Available: http://www.etsi.org

[41] K. Gulati *et al.*, Interference modeling and mitigation toolbox 1.6, for Matlab , ESP Lab., ECE Dept., , Univ. Texas. Austin, TX, USA, Oct. 2011 [Online]. Available: http://users.ece.utexas.edu/bevans/projects/rfi/software/

ICI-Free Equalization in OFDM Systems with Blanking Preprocessing at the Receiver for Impulsive Noise Mitigation

Donatella Darsena, *Member, IEEE*, Giacinto Gelli, Fulvio Melito, and Francesco Verde, *Senior Member, IEEE*

***Abstract*—In this letter, we consider the problem of equalizing finite-impulse response (FIR) channels in orthogonal frequency-division multiplexing (OFDM) systems, which employ at the receiver a blanking nonlinearity to mitigate impulsive noise (IN). By exploiting the frequency redundancy associated with the presence of OFDM virtual carriers, we design a frequency-domain linear FIR equalizer that compensates for the intercarrier interference (ICI) generated by nonlinear preprocessing. Monte Carlo computer simulations, carried out assuming a Middleton Class A model for the IN, allows one to assess the error probability performance of the proposed equalizer.**

***Index Terms*—Blanking nonlinearity, intercarrier interference (ICI) suppression, linear equalization, Middleton Class A noise, orthogonal frequency-division multiplexing (OFDM) systems.**

I. Introduction

TRANSCEIVERS based on orthogonal frequency-division multiplexing (OFDM) have been widely adopted in several wired and wireless standards, including digital subscriber lines [1] and power line communications [2], digital audio [3] and video broadcasting [4], IEEE 802.11 [5] and 802.16 [6], and 3G/4G long term evolution [7]. Such a success is mainly due to the capability of OFDM transceivers to efficiently equalize finite-impulse response (FIR) frequency-selective channels [8]. Indeed, the use of Fast Fourier Transform (FFT) algorithms to perform discrete Fourier transform (DFT) and its inverse (IDFT), coupled with the insertion of a cyclic-prefix (CP), allows one to equalize the FIR channel by means of simple CP removal followed by one-tap frequency-domain equalization (FEQ), provided that the CP length exceeds channel dispersion.

In addition to additive white Gaussian noise (AWGN) and various transceiver implementation losses,[1] potential sources of performance degradation for OFDM systems operating over linear time-invariant channels include narrowband interference (NBI) and impulsive noise (IN). While NBI typically affects only a subset of subcarriers and can be rejected, e.g., by adding suitable constraints to the conventional zero-forcing (ZF) solution [9], [10], [11], [12], [13], [14], [15], [16], [17], [18], [19], [20], *asynchronous* non-Gaussian IN [21], [22], [23], [24], characterized by impulses occurring at the DFT input of the receiver with random arrivals, short duration, and high power, might corrupt *all* the subcarriers within an OFDM symbol and, hence, it is much more difficult to counteract.[2] This fact has recently motivated a vast bulk of research regarding IN characterization and mitigation in OFDM systems (see, e.g., [26], [27], [28], [29], [30], [31], [32], [33], [34]).

A simple strategy to mitigate IN in OFDM systems consists of using at the receiver, before the DFT, a memoryless nonlinearity preprocessor (e.g., clipping, blanking, or a combination thereof) [26], [27]. However, since blanking/clipping is a nonlinear sample-by-sample operation in the time-domain, it distorts the signal constellation and, even worse, destroys orthogonality among OFDM subcarriers, thus resulting into intercarrier interference (ICI) in the frequency-domain. To overcome such a problem, iterative cancellation techniques have been proposed in [28], [29], which nevertheless require *ad hoc* adjustments to avoid slow convergence. An alternative approach [33] is to introduce time diversity at the transmitter by interleaving multiple OFDM symbols after the IDFT and performing symbol-by-symbol blanking at the receiver. In this case, even though linear FIR equalization strategies, e.g., ZF or minimum mean-square error (MMSE) ones, can be used, channel estimation and synchronization must be acquired *before* deinterleaving. On the other hand, instead of employing nonlinear preprocessing at the receiver, it is possible to resort to advanced IN estimation and cancellation methods [30], [34], which exploit the sparsity features of noise in the time-domain. However, also in these cases, the resulting algorithms are iterative and, when compared to the conventional OFDM receiver, a significant computational burden is added.

In this letter, we show that, by exploiting the presence of *virtual carriers* (a solution present in several multicarrier standards), it is possible to design frequency-domain linear FIR

Manuscript received December 09, 2014; accepted January 27, 2015. Date of publication January 29, 2015; date of current version February 12, 2015. The associate editor coordinating the review of this manuscript and approving it for publication was Prof Antonio Marques.

D. Darsena is with the Department of Engineering, Parthenope University, Naples I-80143, Italy (e-mail: darsena@uniparthenope.it).

G. Gelli, F. Melito, and F. Verde are with the Department of Electrical Engineering and Information Technology, University Federico II, Naples I-80125, Italy (e-mail: gelli@unina.it; fulvio.melito@unina.it; f.verde@unina.it).

Color versions of one or more of the figures in this paper are available online at http://ieeexplore.ieee.org.

Digital Object Identifier 10.1109/LSP.2015.2398366

[1]Including time and carrier frequency offsets between the transmitter and the receiver, analog front-end in-phase/quadrature-phase (I/Q) imbalances, and insufficient CP length.

[2]Another type of non-Gaussian IN consists of impulses of longer duration that occur periodically in time (so-called *periodic* IN) [25].

equalizers for channels affected by IN, which are able to compensate for the ICI introduced by a blanking nonlinearity.[3] In particular, a sufficient condition ensuring the existence of such a FIR ICI-free solution is derived. Moreover, it is shown that, with respect to conventional ZF receivers (with or without blanking), a performance gain can be obtained for signal-to-noise ratio (SNR) values of practical interest, with an affordable increase in computational complexity.

A. Asynchronous IN Model

Although the design of the proposed ICI-free equalizer does not rely on specific assumptions about the IN, we briefly describe here the well-known asynchronous Middleton Class A (MCA) model [21]–[23], which will be employed in the numerical performance analysis. A MCA noise sample can be expressed as a complex random variable (RV) $x = g + i$, where g is zero-mean circular symmetric complex Gaussian thermal noise with variance σ_g^2, i.e., $g \in \mathcal{CN}(0, \sigma_g^2)$, whereas i models the non-Gaussian impulse noise with variance σ_i^2. The probability density function of x can be expressed as $p_x(z) = \sum_{n=0}^{+\infty} \alpha_n p_{x|n}(z|n)$, i.e., as a weighted sum of conditionally-Gaussian pdfs $p_{x|n}(z|n) \triangleq \pi^{-1}\sigma_n^{-2}\exp(-|z|^2/\sigma_n^2)$ ($z \in \mathbb{C}$), where $\alpha_n \triangleq e^{-\lambda}\lambda^n/n!$ is the probability that n noise pulses simultaneously occur. For any given $n \in \mathbb{N}$, the parameter σ_n^2 represents the conditional variance of x, which is given by $\sigma_n^2 = \sigma^2\beta_n$, where $\sigma^2 \triangleq \sigma_g^2 + \sigma_i^2$ is the variance of x, whereas $\beta_n \triangleq (n\lambda^{-1} + \Gamma)/(1+\Gamma)$, with $\lambda > 0$ the *impulsive index* and $\Gamma \triangleq \sigma_g^2/\sigma_i^2 > 0$ the *Gaussian ratio*. The two parameters λ and Γ control the degree of impulsiveness of the noise: for $\lambda \ll 1$, the noise becomes more and more impulsive; for $\lambda \geq 1$, the noise tends to be Gaussian. Similarly, for small values of Γ, the noise becomes more impulsive, while it tends to be Gaussian for large values of Γ. Typically, it is assumed that $\Gamma \ll 1$ (see, e.g., [28]).

II. OFDM System Model

We consider a single-user OFDM system employing M subcarriers, M_{uc} of which are utilized, whereas the remaining $M_{\mathrm{vc}} \triangleq M - M_{\mathrm{uc}} > 0$ ones are virtual carriers (VCs). The discrete-time channel between the transmitter and the receiver is modeled as a causal FIR filter with impulse response $h(n)$ ($n \in \mathbb{Z}$), whose order L_h does not exceed the CP length L_{cp}, with $h(0), h(L_h) \neq 0$. Perfect symbol and carrier-frequency synchronization between the transmitter and the receiver is assumed, and channel state information is known only at the receiver via training, but is unknown at the transmitter.

Let $\mathbf{s} \in \mathbb{C}^{M_{\mathrm{uc}}}$ be the data block to be transmitted,[4] we assume that: **(a1)** $\mathbf{s}$ is a zero-mean circularly symmetric complex random vector, with correlation matrix $\mathbb{E}[\mathbf{s}\mathbf{s}^{\mathrm{H}}] = \mathbf{I}_{M_{\mathrm{uc}}}$, and whose entries assume independent and identically distributed (i.i.d.) equiprobable values, e.g., belonging to a quadrature amplitude modulation (QAM) constellation. Let $\mathcal{J}_{\mathrm{uc}} \triangleq \{q_0, q_1, \ldots, q_{M_{\mathrm{uc}}-1}\} \subset \mathcal{J} \triangleq \{0, 1, \ldots, M-1\}$ collect all the indices of the used subcarriers, the symbol block $\mathbf{s}$ is first processed by the full-column rank matrix $\boldsymbol{\Theta} \in \mathbb{R}^{M \times M_{\mathrm{uc}}}$, which inserts the VCs in the arbitrary positions $\mathcal{J}_{\mathrm{vc}} \triangleq \mathcal{J} - \mathcal{J}_{\mathrm{uc}}$. By construction, it results that $\mathbb{E}[||\boldsymbol{\Theta}\mathbf{s}||^2] = 1$. Before being transmitted, the entries of $\boldsymbol{\Theta}\mathbf{s} \in \mathbb{C}^M$ are subject to conventional OFDM processing, encompassing M-point IDFT followed by CP insertion.

At the receiver, after discarding the CP, the time-domain block can be written [8] as

$$\mathbf{r} = \mathbf{H}\mathbf{W}_{\mathrm{IDFT}}\boldsymbol{\Theta}\mathbf{s} + \mathbf{w} \tag{1}$$

where $\mathbf{H} \in \mathbb{C}^{M \times M}$ is a circulant matrix, whose first column is $[h(0), \ldots, h(L_h), 0, \ldots, 0]^{\mathrm{T}}$, $\mathbf{W}_{\mathrm{IDFT}} \in \mathbb{C}^{M \times M}$ is the unitary symmetric IDFT matrix,[5] and $\mathbf{w} \in \mathbb{C}^M$ models the additive noise. It is assumed that: **(a2)** the vector $\mathbf{w} \triangleq [w_0, w_1, \ldots, w_{M-1}]^{\mathrm{T}}$ is independent of $\mathbf{s}$, and its elements are i.i.d. zero-mean RVs with variance $\sigma^2 \triangleq \mathbb{E}[|w_m|^2]$, modeled e.g. as MCA RVs with parameters Γ and λ.

By resorting to standard eigenstructure concepts [35], one has $\mathbf{H} = \mathbf{W}_{\mathrm{IDFT}}\boldsymbol{\mathcal{H}}\mathbf{W}_{\mathrm{DFT}}$ in (1), where the diagonal entries of $\boldsymbol{\mathcal{H}} \triangleq \mathrm{diag}(H_0, H_1, \ldots, H_{M-1})$ are the values of the transfer function $H(z) \triangleq \sum_{n=0}^{L_h} h(n)z^{-n}$ evaluated at the subcarriers $z_m \triangleq \exp[j(2\pi/M)m]$, i.e., $H_m = H(z_m)$, $\forall m \in \mathcal{J}$. We assume that: **(a3)** the channel transfer function $H(z)$ has no zero on the used subcarriers, i.e., $H_m \neq 0$, $\forall m \in \mathcal{J}_{\mathrm{uc}}$.

III. ICI Analysis of Sample-by-sample Blanking

To mitigate the adverse effects of IN, a common strategy is to use sample-by-sample blanking preprocessing [26], [27] in the time-domain, before the conventional OFDM equalizer (i.e., before DFT and FEQ), aimed at discarding those samples of $\mathbf{r}$ that are most contaminated by IN.

Let r_m be the mth ($m \in \mathcal{J}$) sample of $\mathbf{r}$ and $\xi > 0$ denote a suitable threshold, the output of the blanking nonlinearity is $\tilde{y}_m = r_m$ if $|r_m| \leq \xi$, $\tilde{y}_m = 0$ otherwise. Let $\mathcal{B} \triangleq \{m \in \mathcal{J} : |r_m| > \xi\} = \{m_1, m_2, \ldots, m_{|\mathcal{B}|}\}$ denote the subset collecting all the indices of the blanked entries of $\mathbf{r}$; the complement of $\mathcal{B}$ with respect to $\mathcal{J}$ is denoted by $\overline{\mathcal{B}} = \{\overline{m}_1, \overline{m}_2, \ldots, \overline{m}_{|\overline{\mathcal{B}}|}\}$. The input-output relationship of the blanking preprocessor is $\tilde{\mathbf{y}} \triangleq [\tilde{y}_0, \tilde{y}_1, \ldots, \tilde{y}_{M-1}]^{\mathrm{T}} = (\mathbf{I}_M - \mathbf{B})\,\mathbf{r}$, where $\mathbf{B} \triangleq \mathrm{diag}(b_0, b_1, \ldots, b_{M-1})$, with $b_m = 1$ for $m \in \mathcal{B}$, $b_m = 0$ otherwise.

Taking into account (1) and the eigenstructure of $\mathbf{H}$, after DFT one obtains the frequency-domain block $\mathbf{y} \triangleq \mathbf{W}_{\mathrm{DFT}}\tilde{\mathbf{y}} = \mathbf{C}\boldsymbol{\mathcal{H}}\boldsymbol{\Theta}\mathbf{s} + \mathbf{v}$, where $\mathbf{C} \triangleq \mathbf{W}_{\mathrm{DFT}}(\mathbf{I}_M - \mathbf{B})\mathbf{W}_{\mathrm{IDFT}} \in \mathbb{C}^{M \times M}$ and $\mathbf{v} \triangleq \mathbf{W}_{\mathrm{DFT}}(\mathbf{I}_M - \mathbf{B})\mathbf{W} \in \mathbb{C}^M$. It can be verified that $\mathbf{C}$ is a circulant matrix, whose diagonal entries $\{\mathbf{C}\}_{m,m}$ for each $m \in \mathcal{J}$ are equal to $\{\mathbf{C}\}_{m,m} = 1 - |\mathcal{B}|/M = 1 - (M - |\overline{\mathcal{B}}|)/M = |\overline{\mathcal{B}}|/M$, where $|\mathcal{B}|$ and $|\overline{\mathcal{B}}|$ denote the cardinality of $\mathcal{B}$ and $\overline{\mathcal{B}}$, respectively. Consequently, vector $\mathbf{y}$ can be rewritten as

$$\mathbf{y} = \underbrace{\frac{|\overline{\mathcal{B}}|}{M}\boldsymbol{\mathcal{H}}\boldsymbol{\Theta}\mathbf{s}}_{(a)} + \underbrace{\left(\mathbf{C} - \frac{|\overline{\mathcal{B}}|}{M}\mathbf{I}_M\right)\boldsymbol{\mathcal{H}}\boldsymbol{\Theta}\mathbf{s}}_{(b)} + \mathbf{v}. \tag{2}$$

[3] The proposed approach can be extended to other memoryless nonlinearities [27], e.g., clipping or combination of blanking and clipping.

[4] Since all the considered processing is on a symbol-by-symbol basis, for the sake of notation simplicity, we avoid indicating the functional dependence on the symbol interval index.

[5] Its inverse $\mathbf{W}_{\mathrm{DFT}} \triangleq \mathbf{W}_{\mathrm{IDFT}}{}^{-1} = \mathbf{W}_{\mathrm{IDFT}}^*$ is the DFT matrix.

The latter equation shows that the adverse effect of blanking is twofold [29]: (i) reduction of the signal amplitude by a factor $|\overline{\mathcal{B}}|/M$; (ii) introduction of ICI, due to departure of $\mathbf{C}$ from a scaled identity matrix. Indeed, if no entry of $\mathbf{r}$ is blanked, then $|\overline{\mathcal{B}}| = M$ and $\mathbf{C} = \mathbf{I}_M$. In Section IV, we show that these undesired effects of the nonlinearity can be compensated for by a frequency-domain linear FIR equalizer.

IV. Frequency-domain FIR ICI-free Equalization

Consider the problem of recovering the transmitted block $\mathbf{s}$ from the blanking preprocessor output $\mathbf{y}$ after DFT. To this purpose, we employ a frequency-domain linear FIR equalizer, defined by the input-output relationship $\mathbf{x} = \mathbf{F}\mathbf{y}$, with $\mathbf{F} \in \mathbb{C}^{M_{\text{uc}} \times M}$, followed by a minimum-distance decision device. The ICI-free condition leads to the matrix equation $\mathbf{F}\mathbf{C}\boldsymbol{\mathcal{H}}\boldsymbol{\Theta} = \mathbf{I}_{M_{\text{uc}}}$. Such an equation is consistent (i.e., it admits at least one solution) if and only if (iff) $(\mathbf{C}\boldsymbol{\mathcal{H}}\boldsymbol{\Theta})^{-}(\mathbf{C}\boldsymbol{\mathcal{H}}\boldsymbol{\Theta}) = \mathbf{I}_{M_{\text{uc}}}$, with $(\cdot)^{-}$ denoting the generalized (1)-inverse [36]. This condition is fulfilled[6] if $\mathbf{C}\boldsymbol{\mathcal{H}}\boldsymbol{\Theta}$ is full-column rank, i.e., $\text{rank}(\mathbf{C}\boldsymbol{\mathcal{H}}\boldsymbol{\Theta}) = M_{\text{uc}}$. Under this assumption, the *minimal norm* [36] solution of $\mathbf{F}\mathbf{C}\boldsymbol{\mathcal{H}}\boldsymbol{\Theta} = \mathbf{I}_{M_{\text{uc}}}$ is given by $\mathbf{F}_{\text{ICI}-\text{free}} = (\mathbf{C}\boldsymbol{\mathcal{H}}\boldsymbol{\Theta})^{\dagger}$, with $(\cdot)^{\dagger}$ denoting the Moore-Penrose generalized inverse [36].

A. Sufficient Condition for the Existence of ICI-free Solutions

We investigate whether $\text{rank}(\mathbf{C}\boldsymbol{\mathcal{H}}\boldsymbol{\Theta}) = M_{\text{uc}}$ is satisfied, which is a sufficient condition for the existence of ICI-free solutions. To this aim, we provide the following Theorem.

Theorem 1: (Existence of ICI-free solutions): The matrix $\mathbf{C}\boldsymbol{\mathcal{H}}\boldsymbol{\Theta}$ is full-column rank iff $[\boldsymbol{\mathcal{H}}\boldsymbol{\Theta}, \mathbf{W}_{\text{DFT}}\boldsymbol{\Psi}] \in \mathbb{C}^{M \times (M_{\text{uc}}+|\mathcal{B}|)}$ is full-column rank, where $\boldsymbol{\Psi} \triangleq [\mathbf{1}_{m_1}, \mathbf{1}_{m_2}, \ldots, \mathbf{1}_{m_{|\mathcal{B}|}}] \in \mathbb{R}^{M \times |\mathcal{B}|}$, with $\mathbf{1}_m \in \mathbb{R}^M$ denoting the $(m+1)$th column of $\mathbf{I}_M$.

Proof: Since the matrix $\mathbf{W}_{\text{DFT}}$ is nonsingular, it results that $\text{rank}(\mathbf{C}\boldsymbol{\mathcal{H}}\boldsymbol{\Theta}) = \text{rank}[(\mathbf{I}_M - \mathbf{B})\mathbf{W}_{\text{IDFT}}\boldsymbol{\mathcal{H}}\boldsymbol{\Theta}]$. Moreover, by virtue of assumption **(a3)**, one has $\text{rank}(\boldsymbol{\mathcal{H}}\boldsymbol{\Theta}) = M_{\text{uc}}$, which implies that $\text{rank}(\mathbf{W}_{\text{IDFT}}\boldsymbol{\mathcal{H}}\boldsymbol{\Theta}) = M_{\text{uc}}$, since $\mathbf{W}_{\text{IDFT}}$ is a nonsingular matrix. The matrix $(\mathbf{I}_M - \mathbf{B})\mathbf{W}_{\text{IDFT}}\boldsymbol{\mathcal{H}}\boldsymbol{\Theta} \in \mathbb{C}^{M \times M_{\text{uc}}}$ is full-column rank iff [36] $\mathcal{N}(\mathbf{I}_M - \mathbf{B}) \cap \mathcal{R}(\mathbf{W}_{\text{IDFT}}\boldsymbol{\mathcal{H}}\boldsymbol{\Theta}) = \{\mathbf{0}_M\}$. By construction, the mth diagonal entry of $\mathbf{I}_M - \mathbf{B}$ is zero for each $m \in \mathcal{B}$ and, thus, $\text{rank}(\mathbf{I}_M - \mathbf{B}) = M - |\mathcal{B}| = |\overline{\mathcal{B}}|$. Recalling that m_i denotes the ith element of $\mathcal{B}$, for $i \in \{1, 2, \ldots, |\mathcal{B}|\}$, an arbitrary vector $\boldsymbol{\mu} \in \mathbb{C}^M$ belongs to $\mathcal{N}(\mathbf{I}_M - \mathbf{B})$ iff there exists a vector $\boldsymbol{\beta} \in \mathbb{C}^{|\mathcal{B}|}$ such that $\boldsymbol{\mu} = \boldsymbol{\Psi}\boldsymbol{\beta}$, with $\boldsymbol{\Psi} \triangleq [\mathbf{1}_{m_1}, \mathbf{1}_{m_2}, \ldots, \mathbf{1}_{m_{|\mathcal{B}|}}] \in \mathbb{R}^{M \times |\mathcal{B}|}$, where $\mathbf{1}_m \in \mathbb{R}^M$ is the $(m+1)$th column of $\mathbf{I}_M$. Hence, an arbitrary vector $\boldsymbol{\mu} \in \mathcal{N}(\mathbf{I}_M - \mathbf{B})$ also belongs to the subspace $\mathcal{R}(\mathbf{W}_{\text{IDFT}}\boldsymbol{\mathcal{H}}\boldsymbol{\Theta})$ iff there exists a vector $\boldsymbol{\alpha} \in \mathbb{C}^{M_{\text{uc}}}$ such that $\boldsymbol{\Psi}\boldsymbol{\beta} = \mathbf{W}_{\text{IDFT}}\boldsymbol{\mathcal{H}}\boldsymbol{\Theta}\boldsymbol{\alpha}$. As a consequence, condition $\mathcal{N}(\mathbf{I}_M - \mathbf{B}) \cap \mathcal{R}(\mathbf{W}_{\text{IDFT}}\boldsymbol{\mathcal{H}}\boldsymbol{\Theta}) = \{\mathbf{0}_M\}$ holds iff the system of equations $\boldsymbol{\mathcal{H}}\boldsymbol{\Theta}\boldsymbol{\alpha} - \mathbf{W}_{\text{DFT}}\boldsymbol{\Psi}\boldsymbol{\beta} = \mathbf{0}_M$ admits the unique solution $\boldsymbol{\alpha} = \mathbf{0}_{M_{\text{uc}}}$ and $\boldsymbol{\beta} = \mathbf{0}_{|\mathcal{B}|}$. It can be seen [35] that this happens iff the matrix $[\boldsymbol{\mathcal{H}}\boldsymbol{\Theta}, \mathbf{W}_{\text{DFT}}\boldsymbol{\Psi}] \in \mathbb{C}^{M \times (M_{\text{uc}}+|\mathcal{B}|)}$ turns out to be full-column rank. ■

[6]Also the performance of the MMSE equalizer depends on the existence of ICI-free solutions: if $\text{rank}(\mathbf{C}\boldsymbol{\mathcal{H}}\boldsymbol{\Theta}) \neq M_{\text{uc}}$, the error probability performance curve of the MMSE equalizer exhibits a floor when $\sigma^2 \to 0$ [37], [38].

Some remarks are now in order. First, perfect ICI suppression may not be achieved, i.e., $\mathbf{C}\boldsymbol{\mathcal{H}}\boldsymbol{\Theta}$ might not be full-column rank, even if the channel transfer function $H(z)$ has no zero on the used subcarriers [see assumption **(a3)**]. This is due to the fact that the blanking preprocessor introduces ICI in the frequency-domain signal. Only when no entry of $\mathbf{r}$ is blanked, assumption **(a3)** is sufficient for assuring the existence of ICI-free solutions. Second, the fact that some entries of $\mathbf{r}$ are blanked does not prevent perfect ICI compensation. This result stems from the fact that the blanking preprocessor operates in the time-domain (i.e., before the DFT), where each entry of $\mathbf{r}$ is a (noisy) linear combination of all the entries of $\mathbf{s}$. Therefore, if the (m_i)-th sample is blanked, i.e., $b_{m_i} = 1$, the vector $\mathbf{s}$ can still be recovered from the other entries of $\mathbf{r}$. Third, condition $\text{rank}(\mathbf{C}\boldsymbol{\mathcal{H}}\boldsymbol{\Theta}) = M_{\text{uc}}$ amounts to $\text{rank}([\boldsymbol{\mathcal{H}}\boldsymbol{\Theta}, \mathbf{W}_{\text{DFT}}\boldsymbol{\Psi}]) = M_{\text{uc}} + |\mathcal{B}|$, which necessarily requires that $M \geq M_{\text{uc}} + |\mathcal{B}|$ or, equivalently, $M_{\text{vc}} \geq |\mathcal{B}|$. Thus, the number M_{vc} of VCs also represents the maximum number of entries of $\mathbf{r}$ that can be blanked without preventing perfect ICI compensation.

Finally, Theorem 1 does not allow one to determine the threshold ξ (or, equivalently, the blanking subset $\mathcal{B}$), whose choice nevertheless affects the symbol-error-rate (SER) performance of the receiver. Since closed-form analytical evaluation of SER as a function of ξ is a challenging problem,[7] we explore the impact of ξ on SER performance and discuss its choice in Section V by numerical experiments.

B. Computational Complexity

The computational complexity of the $\mathbf{F}_{\text{ICI}-\text{free}}$ equalizer is dominated by calculation of the Moore-Penrose generalized inverse of $\mathbf{C}\boldsymbol{\mathcal{H}}\boldsymbol{\Theta}$. To evaluate such a complexity, observe that the matrix $\mathbf{C}\boldsymbol{\mathcal{H}}\boldsymbol{\Theta}$ is obtained from $\mathbf{C}\boldsymbol{\mathcal{H}} = [\boldsymbol{\zeta}_0, \boldsymbol{\zeta}_1, \ldots, \boldsymbol{\zeta}_{M-1}]$ by picking its columns $\boldsymbol{\zeta}_q \in \mathbb{C}^M$ located on the used subcarrier positions, i.e., for $q \in \mathcal{J}_{\text{uc}}$. It results that $\boldsymbol{\zeta}_q = H_q \sum_{\overline{m} \in \overline{\mathcal{B}}} z_{q\overline{m}} \boldsymbol{\chi}_{\overline{m}}$, where $\boldsymbol{\chi}_{\overline{m}} \triangleq (1/M)[1, z_{\overline{m}}, z_{2\overline{m}} \ldots, z_{(M-1)\overline{m}}]^{\text{H}} \in \mathbb{C}^M$. Let $\mathbf{e}_q \triangleq [z_{q\overline{m}_1}, z_{q\overline{m}_2} \ldots, z_{q\overline{m}_{|\overline{\mathcal{B}}|}}]^{\text{T}} \in \mathbb{C}^{|\overline{\mathcal{B}}|}$, one has $\mathbf{C}\boldsymbol{\mathcal{H}}\boldsymbol{\Theta} = \boldsymbol{\Omega}\mathbf{E}\boldsymbol{\mathcal{H}}_{\text{uc}}$, with $\boldsymbol{\Omega} \triangleq [\boldsymbol{\chi}_{\overline{m}_1}, \boldsymbol{\chi}_{\overline{m}_2}, \ldots, \boldsymbol{\chi}_{\overline{m}_{|\overline{\mathcal{B}}|}}] \in \mathbb{C}^{M \times |\overline{\mathcal{B}}|}$, $\mathbf{E} \triangleq [\mathbf{e}_{q_0}, \mathbf{e}_{q_1}, \ldots, \mathbf{e}_{q_{M_{\text{uc}}-1}}] \in \mathbb{C}^{|\overline{\mathcal{B}}| \times M_{\text{uc}}}$, and $\boldsymbol{\mathcal{H}}_{\text{uc}} \triangleq \text{diag}(H_{q_0}, H_{q_1}, \ldots, H_{q_{M_{\text{uc}}-1}})$. Since $\boldsymbol{\mathcal{H}}_{\text{uc}}$ is nonsingular by virtue of assumption **(a3)** and $\boldsymbol{\Omega}\mathbf{E}$ is full-column rank by construction, i.e., rank $(\boldsymbol{\Omega}\mathbf{E}) = M_{\text{uc}}$, it results [36] that $\mathbf{F}_{\text{ICI}-\text{free}} = \boldsymbol{\mathcal{H}}_{\text{uc}}{}^{-1}(\boldsymbol{\Omega}\mathbf{E})^{\dagger} = M\boldsymbol{\mathcal{H}}_{\text{uc}}{}^{-1}\mathbf{E}^{\dagger}\boldsymbol{\Omega}^{\text{H}}$, where we additionally used the fact that $\boldsymbol{\Omega}^{\text{H}}\boldsymbol{\Omega} = (1/M)\mathbf{I}_{|\overline{\mathcal{B}}|}$.

Compared to the conventional OFDM receiver, the increase in computational complexity for the proposed ICI-free equalizer is due to the calculus of $\mathbf{E}^{\dagger}$. It can be verified that $\mathbf{E}$ is a polynomial Vandermonde matrix [39] with basis polynomials $P_j(x) = x^{q_j}$, for $x \in \mathbb{C}$ and $j \in \{0, 1, \ldots, M_{\text{uc}} - 1\}$, and node points $t_i = z_{m_i}$, for $j \in \{1, 2, \ldots, |\overline{\mathcal{B}}|\}$.[8] Thus, the matrix $\mathbf{E}^{\dagger}$ can be calculated [39] by special fast or superfast algorithms in $\mathcal{O}(M^2)$ or $\mathcal{O}(M \log^2(M))$ floating point operations, respectively.

[7]In principle, following [26], [27], one may choose ξ so as to maximize the signal-to-interference-plus-noise ratio (SINR) at the equalizer output, which is simpler to evaluate. However, since the IN is non-Gaussian, SINR maximization is no longer equivalent to SER minimization.

[8]According to Theorem 1, one has $|\overline{\mathcal{B}}| \geq M_{\text{uc}}$ and rank $(\mathbf{E}) = M_{\text{uc}}$.

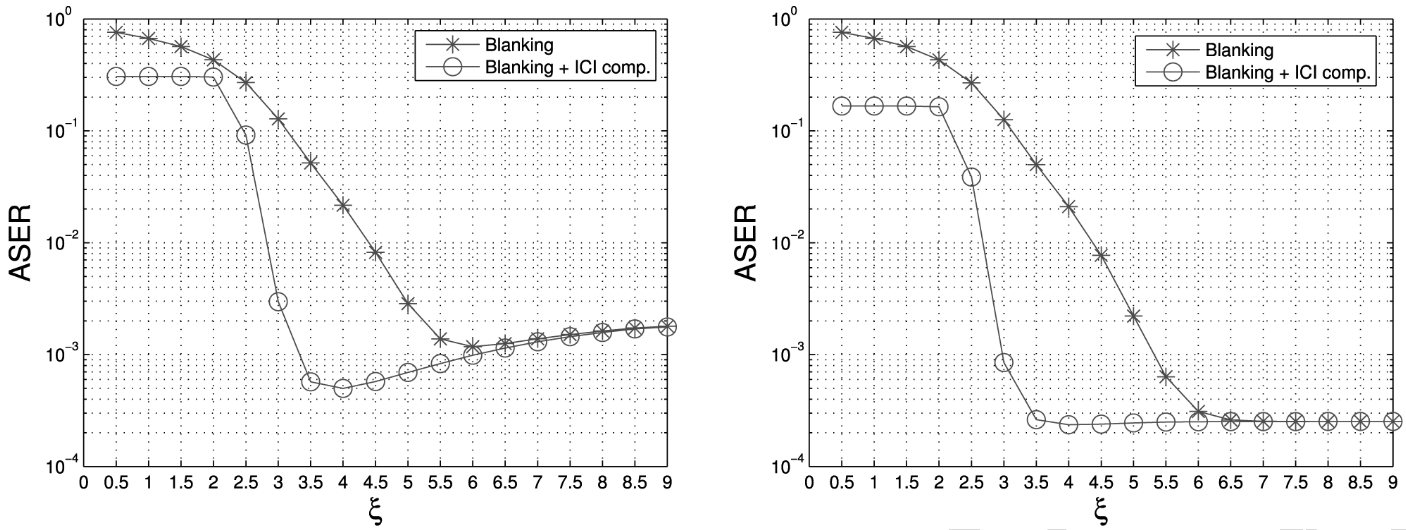

Fig. 1. ASER versus ξ with SNR equal to 15 dB (left-side plot) and 25 dB (right-side plot).

V. Numerical Performance Analysis

The average SER (ASER) performance of the proposed ICI-free receiver (referred to as "Blanking + ICI comp.") was assessed by means of Monte Carlo computer simulations. As a comparison, we also evaluated the ASER performance of: (i) the receiver with blanking nonlinearity followed by conventional ZF equalization, i.e., $\mathbf{F}_{\text{zf}} = (\boldsymbol{\mathcal{H}}\boldsymbol{\Theta})^{\dagger}$ (referred to as "Blanking"); (ii) the conventional OFDM receiver without any nonlinearity preprocessing and ZF equalization (referred to as "Conventional"). With reference to the proposed equalizer, according to Theorem 1, only the M_{vc} entries of $\mathbf{r}$ with largest magnitudes are blanked if $|\mathcal{B}| > M_{\text{vc}}$.

We considered an OFDM system with $M = 32$ subcarriers and a CP length $L_{\text{cp}} = 8$. The system employs $M_{\text{vc}} = 8$ VCs, all located at the edges of the OFDM spectrum, and Gray-labeled 4-QAM signaling for the $M_{\text{uc}} = 24$ utilized subcarriers.[9] The channel impulse response was chosen according to the channel model HiperLAN/2 A (see [40] for details). The MCA impulsive noise was generated by using a modified version of the Matlab toolbox in [41]. We considered a *highly-impulsive* noise scenario with $\lambda = 10^{-3}$ and $\Gamma = 10^{-1}$.

Fig. 1 reports the performance of the two receivers with blanking as a function of the threshold ξ, with SNR $\triangleq 1/\sigma^2 \in \{15, 25\}$ dB. Results show that, as expected, the performance of both receivers depends on the value of the blanking threshold. However, the "Blanking + ICI comp." receiver outperforms the "Blanking" one for all the considered values of ξ, except for very large values of ξ when the entries of $\mathbf{r}$ are not blanked with high probability and, then, the ICI-free equalizer $\mathbf{F}_{\text{ICI-free}}$ boils down to the ZF matrix $\mathbf{F}_{\text{zf}}$.

The ASER performances of all the considered receivers are depicted in Fig. 2 as a function of the SNR. With regard to the receivers employing blanking, we chose the value of ξ minimizing the ASER, for each SNR value. It can be seen that, compared

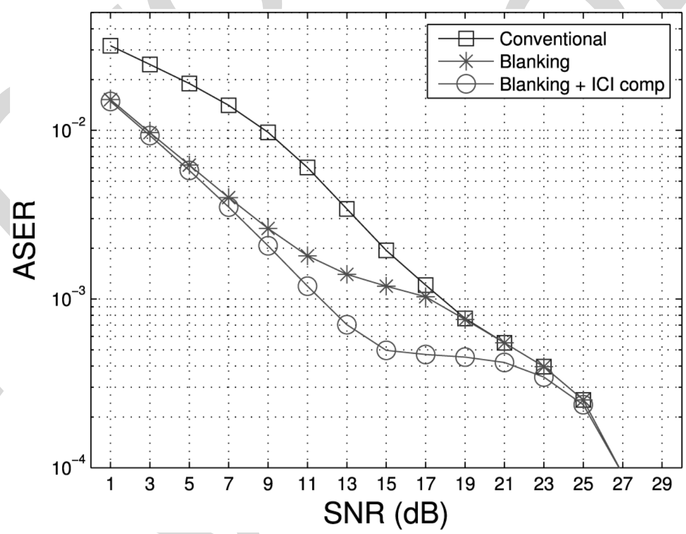

Fig. 2. ASER versus SNR with ξ optimally chosen for each SNR value.

to the conventional OFDM receiver, employing a blanking preprocessing allows one to remarkably improve performances, except for large values of the SNR, for which blanking becomes unlikely and, thus, all the three receivers tend to coincide. Remarkably, the "Blanking+ICI comp." receiver outperforms the "Blanking" one for SNR values of practical interest, ranging from 10 to 20 dB. For instance, for an ASER value of 10^{-3}, the "Blanking + ICI comp." receiver ensures an SNR gain of about 6 dB with respect to the "Blanking" and "Conventional" ones.

VI. Conclusions

By exploiting the redundancy arising from the insertion of VCs in the OFDM signal, we showed that closed-form FIR ICI-free compensation in OFDM receivers, which employ blanking nonlinearity processing to counteract IN, is still feasible. In this case, significant performance gains are obtained with a minor modification of the conventional ZF equalizer.

[9]We performed simulations using a 16-QAM constellation, whose ASER curves are not reported since they show trends similar to the 4-QAM case.

REFERENCES

[1] T. Starr, M. Sorbara, J. M. Cioffi, and P. J. Silverman, *DSL Advances*. Upper Saddle River, NJ, USA: Prentice Hall Professional, 2003.

[2] H. Hrasnica, A. Haidine, and R. Lehnert, *Broadband Powerline Communications*. Hoboken, NJ, USA: Wiley, 2004.

[3] Radio broadcasting systems; Digital audio broadcasting (DAB) to mobile, portable and fixed receivers, ETS Standard 300 401, 1995.

[4] Digital video broadcasting (DVB); Framing structure, channel coding and modulation for digital terrestrial television, ETSI Std. EN 300 744 v1.6.1, 2008.

[5] B. O'Hara and A. Petrick, *The IEEE 802.11 Handbook: A Designer's Companion*. Piscataway, NJ, USA: IEEE Standards, 2005.

[6] IEEE Standard for local and metropolitan area networks Part 16: Air interface for broadband wireless access systems Amendment 3: Advanced air interface, IEEE Std. 802.16 m, 2011.

[7] LTE; Evolved universal terrestrial radio access (E-UTRA) and evolved universal terrestrial radio access network (E-UTRAN); Overall description, 3GPP Std. TS 36.300, 2011.

[8] Z. Wang and G. B. Giannakis, "Wireless multicarrier communications–where fourier meets shannon," *IEEE Signal Process. Mag.*, vol. 17, no. 3, pp. 29–48, May 2000.

[9] D. Darsena, G. Gelli, L. Paura, and F. Verde, "Widely-linear equalization and blind channel identification for interference-contaminated multicarrier systems," *IEEE Trans. Signal Process*, vol. 53, pp. 1163–1177, Mar. 2005.

[10] S. H. Müller-Weinfurtner, "Optimum Nyquist windowing in OFDM receivers," *IEEE Trans. Commun.*, vol. 49, pp. 417–420, Mar. 2002.

[11] D. Darsena, G. Gelli, L. Paura, and F. Verde, "NBI-resistant zero-forcing equalizers for OFDM systems," *IEEE Commun. Lett.*, vol. 9, pp. 744–746, Aug. 2005.

[12] A. J. Redfern, "Receiver window design for multicarrier communication systems," *IEEE J. Sel. Areas Commun.*, vol. 20, pp. 1029–1036, Jun. 2002.

[13] D. Darsena, G. Gelli, L. Paura, and F. Verde, "A constrained maximum-SINR NBI-resistant receiver for OFDM systems," *IEEE Trans. Signal Process.*, vol. 55, pp. 3032–3047, Jun. 2007.

[14] K. Van Acker, G. Leus, M. Moonen, O. van de Wiel, and T. Pollet, "Per tone equalization for DMT-based systems," *IEEE Trans. Commun.*, vol. 49, no. pp, pp. 109–119, Jan. 2001.

[15] K. Van Acker, T. Pollet, G. Leus, and M. Moonen, "Combination of per tone equalization and windowing in DMT-receivers," *Signal Process.*, vol. 81, pp. 1571–1579, Aug. 2001.

[16] D. Darsena, "Successive narrowband interference cancellation for OFDM systems," *IEEE Commun. Lett.*, vol. 11, pp. 73–75, Jan. 2007.

[17] K. Vanbleu, M. Moonen, and G. Leus, "Linear and decision-feedback per tone equalization for DMT-based transmission over IIR channels," *IEEE Trans. Signal Process.*, vol. 54, pp. 258–273, Jan. 2006.

[18] D. Darsena, G. Gelli, and F. Verde, "Universal linear precoding for NBI-proof widely-linear equalization in MC systems," *EURASIP J. Wireless Commun. Netw., Special Issue on Multicarrier Systems*, pp. 1–13, 2008, ID 321450.

[19] S. Trautmann and N. J. Fliege, "A new equalizer for multitone systems without guard time," *IEEE Commun. Lett.*, vol. 6, pp. 34–36, Jan. 2002.

[20] D. Darsena and F. Verde, "Successive NBI cancellation using soft decisions for OFDM systems," *IEEE Signal Process. Lett.*, vol. 15, pp. 873–876, 2008.

[21] D. Middleton, "Statistical-physical models of electromagnetic interference," *IEEE Trans. Electromagn. Compat.*, vol. 19, pp. 106–127, Aug. 1977.

[22] A. D. Spaulding and D. Middleton, "Optimum reception in the impulse interference environment–part I: Coherent detection," *IEEE Trans. Commun.*, vol. 25, pp. 910–923, Sep. 1977.

[23] D. Middleton, "Procedure for determining the parameters of a first-order canonical models of class A and class B electromagnetic interference," *IEEE Trans. Electromagn. Compat.*, vol. 21, pp. 190–208, Aug. 1979.

[24] P. A. Delaney, "Signal detection in multivariate class-A interference," *IEEE Trans. Commun.*, vol. 43, pp. 365–373, Feb. 2006.

[25] M. Nassar, A. Dabak, I. Kim, T. Pande, and B. L. Evans, "Cyclostationary noise modeling in narrowband powerline communication for smart grid application," in *Proc. IEEE Int. Conf. on Acoustics, Speech and Sig. Proc.*, Kyoto, Japan, Mar. 2012, pp. 3089–3092.

[26] S. V. Zhidkov, "Performance analysis and optimization of OFDM receiver with blanking nonlinearity in impulsive noise environment," *IEEE Trans. Veh. Technol.*, vol. 55, pp. 234–242, Jan. 2006.

[27] S. V. Zhidkov, "Analysis and comparison of several simple impulse noise mitigation schemes for OFDM receivers," *IEEE Trans. Commun.*, vol. 56, pp. 5–9, Jan. 2008.

[28] A. Mengi and A. Vinck, "Successive impulse noise suppression in OFDM," in *Proc. 2010 IEEE Int. Symp. Power Line Communications and Its Applications*, Rio de Janeiro, Brazil, Mar. 2010, pp. 33–37.

[29] C.-H. Yih, "Iterative interference cancellation for OFDM signals with blanking nonlinearity in impulsive noise channels," *IEEE Signal Process. Lett.*, vol. 19, pp. 147–150, Mar. 2012.

[30] J. Lin, M. Nassar, and B. L. Evans, "Impulsive noise mitigation in powerline communications using sparse Bayesian learning," *IEEE J. Sel. Areas Commun.*, vol. 31, pp. 1172–1183, Jul. 2013.

[31] R. Savoia and F. Verde, "Performance analysis of distributed space-time block coding schemes in Middleton class a noise," *IEEE Trans. Veh. Technol.*, vol. 62, pp. 2579–2595, Jul. 2013.

[32] D. Darsena, G. Gelli, F. Melito, and F. Verde, "Impulse noise mitigation for MIMO-OFDM wireless networks with linear equalization," in *Proc. IEEE Int. Workshop on Measurements and Networking (M&N)*, Naples, Italy, Oct. 2013, pp. 94–99.

[33] M. Mirahmadi, A. Al-Dweik, and A. Shami, "BER reduction of OFDM based broadband communication systems over multipath channels with impulsive noise," *IEEE Trans. Commun.*, vol. 61, pp. 4602–4615, Nov. 2013.

[34] T. Y. Al-Naffouri, A. A. Quadeer, and G. Caire, "Impulsive noise estimation and removal for OFDM systems," *IEEE Trans. Commun.*, vol. 62, pp. 976–989, Mar. 2014.

[35] R. A. Horn and C. R. Johnson, *Matrix Analysis*. Cambridge, U.K.: Cambridge Univ. Press, 1990.

[36] A. Ben-Israel and T. N. E. Greville, *Generalized Inverses*. New York, NY, USA: Springer-Verlag, 2002.

[37] F. Verde, "Subspace-based blind multiuser detection for quasi-synchronous MC-CDMA systems," *IEEE Signal Process. Lett.*, vol. 11, pp. 621–624, Jul. 2004.

[38] A. S. Cacciapuoti, G. Gelli, and F. Verde, "FIR zero-forcing multiuser detection and code designs for downlink MC-CDMA," *IEEE Trans. Signal Process.*, vol. 55, pp. 4737–4751, Oct. 2007.

[39] V. Y. Pan, *Structured Matrices and Polynomials: Unified Superfast Algorithms*. Boston, MA, USA: Birkhäuser, 2001.

[40] ETSI Normalization Committee, Channel models for HIPERLAN/2 in different indoor scenarios, [Online]. Available: http://www.etsi.org

[41] K. Gulati *et al.*, Interference modeling and mitigation toolbox 1.6, for Matlab , ESP Lab., ECE Dept., , Univ. Texas. Austin, TX, USA, Oct. 2011 [Online]. Available: http://users.ece.utexas.edu/bevans/projects/rfi/software/